Acta Physica Hungarica 74 (4), pp. 329–339 (1994)

SUB-DOPPLER OPTICAL–OPTICAL DOUBLE RESONANCE POLARIZATION SPECTROSCOPY AND COLLISIONAL ENERGY TRANSFER*

SHUNJI KASAHARA, HEIJI IKOMA and HAJIME KATÔ

Department of Chemistry, Faculty of Science, Kobe University
Nada-ku, Kobe 657, Japan

(Received 26 April 1994)

Sub-Doppler optical-optical double resonance polarization spectroscopy is applied to study highly excited states of NaK molecule. New three $^1\Delta$ states and two $^1\Sigma^+$ states are identified and the molecular constants are determined. Transitions from rotationally energy transferred levels are observed, and this indicates the strong conservation of M_J through the energy transfer by collisions. The linewidths are found to increase with ΔJ, and this implies that the velocity vector approaches to the thermal distribution as ΔJ increases.

1. Introduction

Laser labeling techniques [1–5] are very useful to study the molecular states in high density of levels, because only transitions from the well defined rovibronic (rotational–vibrational–electronic) levels labeled by a pump laser are observed. When a monochromatic pump laser is tuned to the center of the Doppler profile of an absorption line, only molecules with zero component of velocity along the propagation vector of a pump laser are excited. Polarization labeling [2–5] uses an optical anisotropy in the upper and lower levels pumped by a linearly or circularly polarized light. If a linearly polarized probe laser is tuned to be resonant with an optical transition involving the level labeled by the pump laser, the probe beam undergoes a change in the polarization and can pass through a crossed polarizer placed after the absorption cell. The optical–optical double resonance polarization spectroscopy (OODRPS), which uses two single mode lasers, is essentially Doppler-free and is superior in signal-to-noise than other saturation spectroscopies [4,5].

In a hetero-nuclear diatomic molecule, the gerade and ungerade symmetry in a homonuclear diatomic molecule disappears and the more electronic transitions become allowed. Highly excited states of $^{23}Na^{39}K$ were studied by the sub-Doppler OODRPS using two dye lasers [6]. We have extended the study to the rovibronic levels in the 31250–31790 cm^{-1} region, which are observed by the sub-Doppler OODRPS using a Titanium : Sapphire laser and a dye laser, and the results are reported in this paper. New three $^1\Delta$ states and two $^1\Sigma^+$ states are identified,

* Dedicated to Professor István Kovács on his eightieth birthday

and the vibrational and rotational constants are determined. In the OODRPS, predominantly three types (I, II and III in Fig. 1) of probe signals are observed. In addition to these, the modified types (IV, V and VI in Fig. 1) are observed. Type IV is a transition from the levels populated by a resonance fluorescence. The lines of types V and VI, which are induced by collisions, are observed as the satellite lines of predominant lines of types I–III. From the energy spacings of the satellite lines, we can identify whether the transitions are from the neighboring rotational levels of the ground level or of the excited level. Not only the line intensity but also the lineshape and linewidth are observed to change with the change of the rotational quantum number ΔJ. These results are reported in this article.

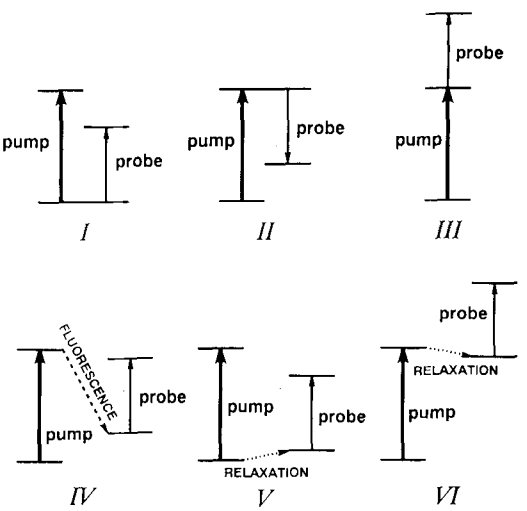

Fig. 1. The six types of optical–optical double resonance, produced by laser saturation of an absorption line

2. Experimental

NaK vapor was produced by heating a 1 : 4 mixture of sodium and potassium metals in a stainless steel heat pipe oven, which was operated at 575 K with a buffer gas of 0.5 Torr Ar. The vapor pressures of Na, K, Na_2, K_2 and NaK at 575 K are estimated to be about 0.015, 0.30, 1.5×10^{-4}, 1.1×10^{-3} and 0.9×10^{-3} Torr, respectively.

The experimental set-up is schematically shown in Fig. 2. The output of a pump laser (Ring laser 1: Coherent CR699-29 dye laser, linewidth 500 kHz) was split into a linearly polarized weak probe beam and a circularly polarized or a linearly

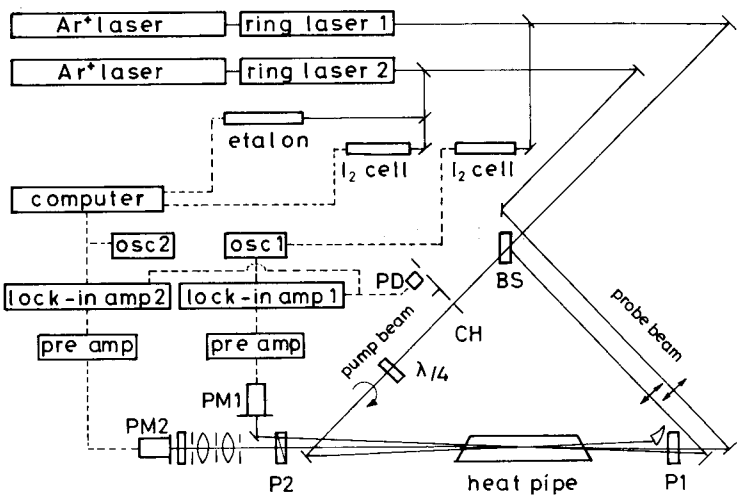

Fig. 2. Experimental arrangement of sub-Doppler optical–optical double resonance polarization spectroscopy. BS is a beam splitter, CH is a chopper, and PD is a photo diode

polarized (at 45° to the probe polarization) strong pump beam. Two beams passed in opposite directions through a heat pipe. If the monochromatic laser is tuned, only the molecules with zero component of velocity along the beam direction can absorb both beams. The linearly polarized weak beam, which passes a linear polarizer P1, cannot pass through a crossed linear polarizer P2. If the weak beam is absorbed by the molecules which can absorb the pump beam, the polarization is altered from a linear to a slightly elliptical polarization. Then, the beam passes the crossed linear polarizer P2 and can reach a photomultiplier PM1 (Hamamatsu R712). The pump beam was modulated by a chopper (3 kHz), and the signal output was detected by a lock-in amplifier 1 (PAR 128A). The pump beam was fixed to a center of Doppler-free line of a known transition $B^1\Pi(v', J') - X^1\Sigma^+(v'', J'')$. The output of a probe laser (Ring laser 2: Coherent CR899-29 Titanium : Sapphire laser or CR699-29 dye laser, lindewidth 500 kHz), which passes a linear polarizer P1, is propagated in the opposite direction to the strong pump beam through the heat pipe. When the probe laser is tuned, the polarization is altered if the frequency of the probe laser coincides with a center of the Doppler profile of transition lines which share a common level with the pump transition. Then, the probe beam passes the crossed linear polarizer P2 and reaches a photomultiplier PM2 (Hamamatsu R636). The

signal output was detected by a lock-in amplifier 2 (EG&G model 5210). In order to confirm that the pump laser stayed on the center frequency of a selected transition, the signal of PM1 was monitored. Thus, the OODRPS spectrum could be obtained without either Doppler broadening or Doppler shift. The absolute wavenumber $\tilde{\nu}$ of the observed spectral line was calibrated by the spectra of iodine: the absorption spectrum for the iodine vapor at 600 K with the path length of 8 m was used to calibrate $\tilde{\nu}$ of a Titanium : Sapphire laser, and the fluorescence excitation spectrum was used to calibrate $\tilde{\nu}$ of a dye laser. The fringe patterns of a confocal etalon (FSR = 150 MHz) were used as a frequency marker.

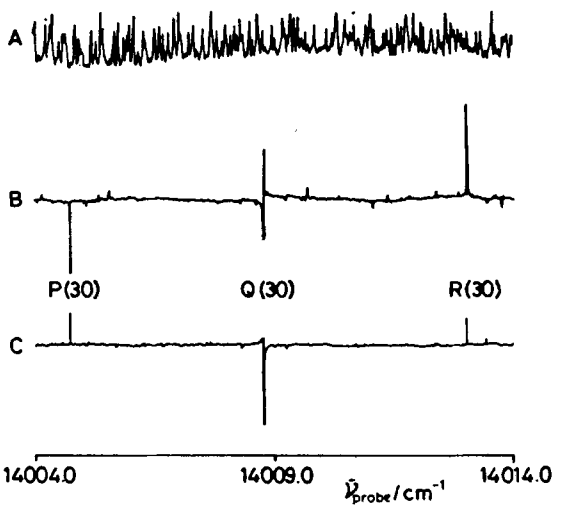

Fig. 3. Optical–optical double resonance polarization spectra around the $A^1\Delta(v_a + 3, J = 29, 30, 31) \leftarrow B^1\Pi(v' = 8, J' = 30)$ transitions. **A** is an absorption spectrum of iodine. **B** is the OODRPS spectrum pumped by a linearly polarized beam. The pump laser is fixed to the $B^1\Pi(v' = 8, J' = 30e) \leftarrow X^1\Sigma^+(v'' = 0, J'' = 31e)$ transition. **C** is the OODRPS spectrum pumped by a circularly polarized beam. The pump laser is fixed to the $B^1\Pi(v' = 8, J' = 30f) \leftarrow X^1\Sigma^+(v'' = 0, J'' = 30e)$ transition

3. Results and discussion

A part of the OODRPS spectra, which contains the $^1\Delta(v, J = 29, 30, 31) - B^1\Pi(v' = 8,\ J' = 30)$ transitions, is shown in Fig. 3. When the pump laser is fixed to an assigned transition $B^1\Pi(v', J') - X^1\Sigma^+(v'', J'')$, only $^1\Sigma^+$, $^1\Sigma^-$, $^1\Pi$ and $^1\Delta$ states can be excited by an electric dipole transition. The formulas for relative transition intensities for the two-step polarization-labeling spectroscopy of diatomic

molecules were derived by Carlson et al [3] and those for the OODRPS are similar. From the pattern of spectral lines, we can identify the symmetry of the excited state. When a circularly polarized pump beam is fixed to a P or R line, the P and R lines can be detected as Lorentzian lines with different signs for the $^1\Sigma^+ - {}^1\Pi$, $^1\Pi - {}^1\Pi$, and $^1\Delta - {}^1\Pi$ transitions. If the polarization of the pump beam is slightly elliptical, the Q lines can also be detected as a dispersed line for the $^1\Sigma^- - {}^1\Pi$ and $^1\Delta - {}^1\Pi$ transitions. On the other hand, when the pump beam polarized linearly at 45° to the probe polarization is fixed to a Q line, Q lines can be detected for the $^1\Sigma^+ - {}^1\Pi$ and $^1\Delta - {}^1\Pi$ transitions, and weak P and R lines can also be detected as Lorentzian lines with the same signs for the $^1\Sigma^- - {}^1\Pi$, $^1\Pi - {}^1\Pi$ and $^1\Delta - {}^1\Pi$ transitions. The intensity of Q line of the $^1\Pi - {}^1\Pi$ transitions is proportional to J^{-2} and the Q lines can be detected at only low J. Using these characters, we have identified three $^1\Delta$ states and two $^1\Sigma^+$ states in the 31250–31790 cm^{-1} region.

The term energy of an excited level $\Lambda(v, J)$, which is excited by a two-step absorption

$$\Lambda(v, J) \overset{h\nu_2}{\text{—}} B^1\Pi(v', J') \overset{h\nu_1}{\text{—}} X^1\Sigma^+(v'', J'') \tag{1}$$

is obtained as a sum of $h\nu_1$, $h\nu_2$, and the term energy of the $X^1\Sigma^+(v'', J'')$ level which is calculated from the molecular constants [7]. The assigned lines and the term energies of upper levels are listed in Table I. The term energy of a rotational–vibrational level is expressed as [8]

Table I

Assigned lines of the $^1\Lambda(v, J) - B^1\Pi(v', J')$ transitions of $^{23}Na^{39}K$, and term energies $E(v, J)$ of upper levels $^1\Lambda(v, J)$. The $B^1\Pi(v', J'e)$ level is excited by a P line. The $B^1\Pi(v', J'f)$ level is excited by a Q line

$^1\Lambda(v, J)$	$B^1(v', J')$	Line energy	$E(v, J)$
$A^1\Delta(v_a, 29e)$	8, 30e	13747.5295	31318.9800
$A^1\Delta(v_a, 30f)$	8, 30e	13751.7654	31323.2159
$A^1\Delta(v_a, 31e)$	8, 30e	13756.0763	31327.5268
$A^1\Delta(v_a, 29f)$	8, 30f	13747.5954	31319.0486
$A^1\Delta(v_a, 30e)$	8, 30f	13751.7303	31323.1835
$A^1\Delta(v_a, 31f)$	8, 30f	13756.0948	31327.5480
$A^1\Delta(v_a + 1, 29e)$	8, 30e	13833.6081	31405.0586
$A^1\Delta(v_a + 1, 30f)$	8, 30e	13837.7803	31409.2308
$A^1\Delta(v_a + 1, 31e)$	8, 30e	13842.0840	31413.5345
$A^1\Delta(v_a + 2, 29e)$	8, 30e	13919.3403	31490.7908
$A^1\Delta(v_a + 2, 30f)$	8, 30e	13923.4657	31494.9162
$A^1\Delta(v_a + 2, 31e)$	8, 30e	13927.7427	31499.1932
$A^1\Delta(v_a + 3, 29e)$	8, 30e	14004.6948	31576.1453
$A^1\Delta(v_a + 3, 30f)$	8, 30e	14008.7878	31580.2383
$A^1\Delta(v_a + 3, 31e)$	8, 30e	14013.0130	31584.4635
$A^1\Delta(v_a + 4, 29e)$	9, 30e	14040.3992	31660.9571
$A^1\Delta(v_a + 4, 30f)$	9, 30e	14044.4463	31665.0042
$A^1\Delta(v_a + 4, 31e)$	9, 30e	14048.6242	31669.1821
$A^1\Delta(v_a + 5, 29e)$	8, 30e	14173.3940	31744.8445
$A^1\Delta(v_a + 5, 30f)$	8, 30e	14177.3853	31748.8358
$A^1\Delta(v_a + 5, 31e)$	8, 30e	14181.5056	31752.9561

Table I (continued)

$^1\Lambda(v, J)$	$B^1(v', J')$	Line energy	$E(v, J)$
$B^1\Delta(v_b\ \ ,29e)$	$8,30e$	13782.2784	31353.7289
$B^1\Delta(v_b\ \ ,30f)$	$8,30e$	13786.3490	31357.7995
$B^1\Delta(v_b\ \ ,31e)$	$8,30e$	13790.5517	31362.0022
$B^1\Delta(v_b+1,27e)$	$8,28e$	13867.4954	31431.8028
$B^1\Delta(v_b+1,28f)$	$8,28e$	13871.2823	31435.5897
$B^1\Delta(v_b+1,29e)$	$8,28e$	13875.2050	31439.5124
$B^1\Delta(v_b+1,29e)$	$8,30e$	13868.0636	31439.5141
$B^1\Delta(v_b+1,30f)$	$8,30e$	13872.1165	31443.5670
$B^1\Delta(v_b+1,31e)$	$8,30e$	13876.3125	31447.7630
$B^1\Delta(v_b+2,29e)$	$8,30e$	13952.7421	31524.1926
$B^1\Delta(v_b+2,30f)$	$8,30e$	13956.7859	31528.2364
$B^1\Delta(v_b+2,31e)$	$8,30e$	13960.9741	31532.4246
$B^1\Delta(v_b+3,29e)$	$8,30e$	14036.4539	31607.9044
$B^1\Delta(v_b+3,30f)$	$8,30e$	14040.4889	31611.9394
$B^1\Delta(v_b+3,31e)$	$8,30e$	14044.6868	31616.1373
$B^1\Delta(v_b+4,29e)$	$8,30e$	14119.6835	31691.1340
$B^1\Delta(v_b+4,30f)$	$8,30e$	14123.7225	31695.1730
$B^1\Delta(v_b+4,31e)$	$8,30e$	14127.9312	31699.3817
$B^1\Delta(v_b+5,27e)$	$8,28e$	14202.6433	31766.9507
$B^1\Delta(v_b+5,28f)$	$8,28e$	14206.4149	31770.7223
$B^1\Delta(v_b+5,29e)$	$8,28e$	14210.3764	31774.6838
$B^1\Delta(v_b+5,29e)$	$8,30e$	14203.2350	31774.6855
$B^1\Delta(v_b+5,30f)$	$8,30e$	14207.2787	31778.7292
$B^1\Delta(v_b+5,31e)$	$8,30e$	14211.5069	31782.9574
$C^1\Delta(v_c\ \ ,29e)$	$8,30e$	14112.6068	31684.0573
$C^1\Delta(v_c\ \ ,30f)$	$8,30e$	14116.5242	31687.9747
$C^1\Delta(v_c\ \ ,31e)$	$8,30e$	14120.9484	31692.3989
$C^1\Delta(v_c+1,27e)$	$8,28e$	14196.3785	31760.6859
$C^1\Delta(v_c+1,28f)$	$8,28e$	14200.0845	31764.3919
$C^1\Delta(v_c+1,29e)$	$8,28e$	14204.0881	31768.3955
$C^1\Delta(v_c+1,29e)$	$8,30e$	14196.9462	31768.3967
$C^1\Delta(v_c+1,30f)$	$8,30e$	14200.9043	31772.3548
$C^1\Delta(v_c+1,31e)$	$8,30e$	14205.2117	31776.6622
$D^1\Sigma(v_d\ \ ,27e)$	$8,28e$	13812.3147	31376.6221
$D^1\Sigma(v_d\ \ ,29e)$	$8,28e$	13819.0606	31383.3680
$D^1\Sigma(v_d\ \ ,29e)$	$8,30e$	13811.9170	31383.3675
$D^1\Sigma(v_d\ \ ,31e)$	$8,30e$	13819.1182	31390.5687
$D^1\Sigma(v_d\ \ ,30e)$	$8,30f$	13815.4455	31386.8987
$D^1\Sigma(v_d+1,27e)$	$8,28e$	13867.7401	31432.0475
$D^1\Sigma(v_d+1,29e)$	$8,28e$	13874.4639	31438.7713
$D^1\Sigma(v_d+1,29e)$	$8,30e$	13867.3247	31438.7752
$D^1\Sigma(v_d+1,31e)$	$8,30e$	13874.5192	31445.7897
$D^1\Sigma(v_d+1,30e)$	$8,30f$	13870.8602	31442.3134
$D^1\Sigma(v_d+2,29e)$	$8,28e$	13929.2177	31493.5251
$D^1\Sigma(v_d+2,29e)$	$8,30e$	13922.0738	31493.5243
$D^1\Sigma(v_d+2,31e)$	$8,30e$	13929.2630	31500.7135
$D^1\Sigma(v_d+2,30e)$	$8,30f$	13925.6077	31497.0609
$D^1\Sigma(v_d+3,29e)$	$8,30e$	13978.6600	31550.1105
$D^1\Sigma(v_d+3,31e)$	$8,30e$	13985.8289	31557.2794
$D^1\Sigma(v_d+3,30e)$	$8,30f$	13982.1635	31553.6167

Table I (continued)

$^1\Lambda(v, J)$	$B^1(v', J')$	Line energy	$E(v, J)$
$E^1\Sigma(v_d, 27e)$	$8, 28e$	13775.6443	31339.9517
$E^1\Sigma(v_d, 29e)$	$8, 28e$	13782.2657	31346.5731
$E^1\Sigma(v_d, 29e)$	$8, 30e$	13775.1274	31346.5779
$E^1\Sigma(v_d, 31e)$	$8, 30e$	13782.2286	31353.6791
$E^1\Sigma(v_d, 30e)$	$8, 30f$	13778.6138	31350.0670
$E^1\Sigma(v_d + 1, 27e)$	$8, 28e$	13831.1831	31395.4905
$E^1\Sigma(v_d + 1, 29e)$	$8, 28e$	13838.6211	31402.9285
$E^1\Sigma(v_d + 1, 29e)$	$8, 30e$	13831.4776	31402.9281
$E^1\Sigma(v_d + 1, 31e)$	$8, 30e$	13838.5497	31410.0002
$E^1\Sigma(v_d + 1, 30e)$	$8, 30f$	13834.9607	31406.4139

$$E(v, J) = E_v + B_v[J(J+1) - \Lambda^2] + \ldots, \tag{2}$$

where $\Lambda = 0, \pm 1$, and ± 2, respectively for Σ, Π and Δ states. E_v is the vibrational energy and B_v is the rotational constant. These constants are determined, and the results are listed in Table II. From the values of E_v, B_v and the vibrational spacing $\Delta G_v = E_{v+1} - E_v$, the excited states are classified. The vibrational quantum numbers $v_x (x = a \sim e)$ could not be assigned.

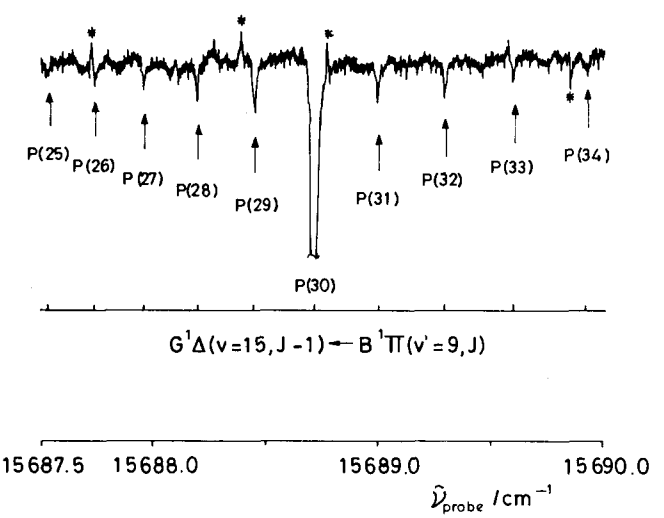

Fig. 4. A part of the optical–optical double resonance polarization spectrum. Around the strong line of the $G^1\Delta(v = 15, J = 29e) \leftarrow B^1\Pi(v' = 9, J' = 30e)$ transition, the transition lines from rotationally energy transferred levels are observed. The pump laser is fixed to the $B^1\Pi(v' = 9, J' = 30e) \leftarrow X^1\Sigma^+(v'' = 0, J'' = 31e)$ transition. The molecular constants of the $G^1\Delta$ state are reported in Ref. [6]

Table II
Molecular constants of the $A^1\Delta$, $B^1\Delta$, $C^1\Delta$, $D^1\Sigma^+$ and $E^1\Sigma^+$ states of $^{23}Na^{29}K$. All values are in units of cm^{-1}. The notations $A, B, C, \ldots$ are tentative

State	v	E_v	ΔG_v	$10^2 B_v$
$A^1\Delta$	v_a	31258.312	86.582	7.0056
$A^1\Delta$	v_a+1	31344.894	86.254	6.9475
$A^1\Delta$	v_a+2	31431.148	85.952	6.8872
$A^1\Delta$	v_a+3	31517.100	85.468	6.8182
$A^1\Delta$	v_a+4	31602.568	84.697	6.7418
$A^1\Delta$	v_a+5	31687.265		6.6489
$B^1\Delta$	v_b	31295.002	85.958	6.7814
$B^1\Delta$	v_b+1	31380.960	84.799	6.7614
$B^1\Delta$	v_b+2	31465.759	83.705	6.7475
$B^1\Delta$	v_b+3	31549.464	83.125	6.7483
$B^1\Delta$	v_b+4	31632.589	83.380	6.7604
$B^1\Delta$	v_b+5	31715.969		6.7802
$C^1\Delta$	v_c	31624.846	84.879	6.8374
$C^1\Delta$	v_c+1	31709.725		6.7750
$D^1\Sigma$	v_d	31332.015	55.455	5.9026
$D^1\Sigma$	v_d+1	31387.470	54.787	5.8971
$D^1\Sigma$	v_d+2	31442.257	56.731	5.8928
$D^1\Sigma$	v_d+3	31498.988		5.8761
$E^1\Sigma$	v_e	31295.938	56.558	5.8207
$E^1\Sigma$	v_e+1	31352.496		5.7968

Collisionally induced satellite lines in the fluorescence spectra were used to study the relaxation between rotational levels of electronically excited molecules [9,10]. The lineshapes of the satellite lines of Li_2 excited to the $A^1\Sigma^+(v'=16, J'=6)$ level were studied by using a technique of the optical–optical double resonance saturation spectroscopy (OODRSS) [11]. In the OODRPS spectrum, the satellite lines of excited molecules are observed around the spectral lines of types II and III. When the pump laser is fixed to the $B^1\Pi(v'=9, J'=30e) \leftarrow X^1\Sigma^+(v''=0, J''=31e)$ transition, the transition lines from rotationally energy transferred levels are observed around the strong line of the $G^1\Delta(v=15, J=29e) \leftarrow B^1\Pi(v'=9, J'=30e)$ transition (see Fig. 4). The lines of $|\Delta J|$ up to 5 are observed, and the intensities of satellite lines decrease as ΔJ increases. This implies strong conservation of M_J throughout energetic inelastic collisions, where M_J is the component of J along the quantization axis. This is consistent with the previous finding that a very high degree of polarization is preserved for iodine fluorescence from rotationally transferred levels [12]. The linewidths Γ(FWHM) are observed to increase as $|\Delta J|$ increases (see Fig. 5). This implies that the rotationally transferred molecules get velocity along the propagation vector of the probe beam and the velocity change increases as $|\Delta J|$ increases.

Similar and more strong spectra are observed for the transitions from nearby levels of the depopulated $X^1\Sigma^+(v'', J'')$ level. The relative intensities and some line spectra are shown in Fig. 6. A monochromatic pump laser is tuned to excite only

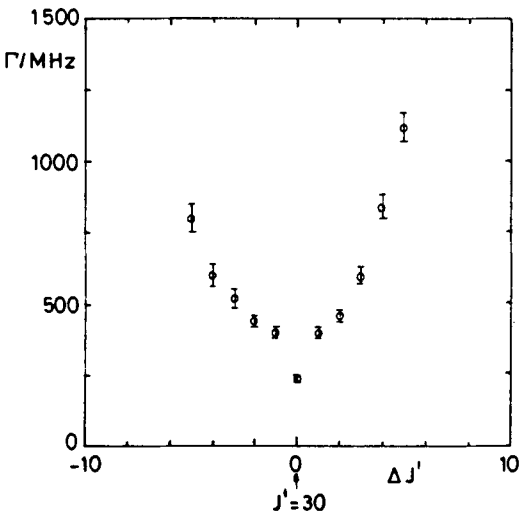

Fig. 5. Linewidths Γ(FWHM) of the $G^1\Delta(v = 15, J = 29 + \Delta J') \leftarrow B^1\Pi(v' = 9, J' = 30 + \Delta J')$ transitions are plotted against $\Delta J'$

molecules with zero component of velocity along the propagation vector, and the polarized pump beam depopulates a chosen $X^1\Sigma^+(v'', J'')$ level anisotropically in $M_{J''}$. Let us call this depopulated level a hole (v'', J''). The observed spectrum indicates that the hole $(v'' = 0, J'' = 17)$ transfers to the neighboring levels by collisions, and the transition lines up to $\Delta J'' = 50$ are observed. In thermal equilibrium at 575 K, the most highly populated level in the $X^1\Sigma^+(v'' = 0)$ state is calculated to be $J'' = 54$. When the $J'' = 17$ level is depopulated, the intensity of $\Delta J'' > 0$ line is observed to be larger than the one of $\Delta J'' < 0$ line. This can be explained as the distribution of the hole tends to be thermal distribution through collisions. The linewidths of the probe transitions $B^1\Pi(v' = 4, J' = J'' \pm 1) - X^1\Sigma^+(v'' = 0, J'' = 17 + \Delta J'')$ are plotted against $\Delta J''$ in Fig. 7. The linewidth Γ is observed to increase with $\Delta J''$, and $\Gamma = 1$ GHz at $\Delta J'' = 40$. The Doppler width of NaK molecule in the thermal equilibrium at 575 K is evaluated to be about 1.1 GHz. This implies that the velocity distribution becomes almost in thermal equilibrium at $\Delta J'' \geq 40$, but the $M_{J''}$ is still fairly conserved.

The collisional energy transfer between the rotational levels in the excited state $B^1\Pi$ can occur when the excited molecule collides before it relaxes to the ground state by radiating a photon. The lifetime of the $B^1\Pi(v' = 4, J')$ level is reported to be 15 ns [13]. If the cross-section of the rotational energy transfer by collision with the K atom is estimated to be 10^3 Å^2, the excited molecule experiences about 0.5 times the collision at 575 K while it stays in the excited state. On the

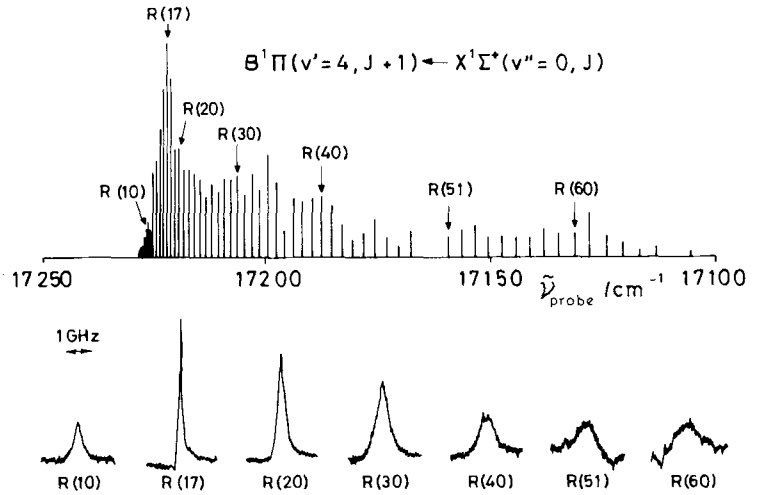

Fig. 6. Intensity distribution of the probe transitions $B^1\Pi(v' = 4, J' = J'' + 1) \leftarrow X^1\Sigma^+(v'' = 0, J'' = 17+\Delta J'')$. The pump laser is fixed to the $B^1\Pi(v' = 6, J' = 18) \leftarrow X^1\Sigma^+(v'' = 0, J'' = 17)$ transition. Some line spectra are shown below

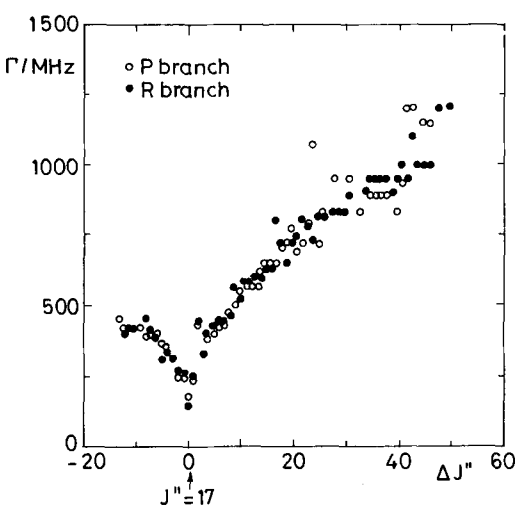

Fig. 7. Linewidths Γ(FWHM) of the $B^1\Pi(v' = 4, J' = J''\pm1) \leftarrow X^1\Sigma^+(v'' = 0, J'' = 17+\Delta J'')$ transitions are plotted against $\Delta J''$. The ones of P and R branches are plotted, respectively, by an open circle (o) and a closed circle (•)

other hand, the collisional transfer of the hole between the rotational levels in the ground state $X^1\Sigma^+$ can be observed by the OODRPS as long as the holes retain an anisotropy in $M_{J''}$. Because of strong conservation of M_J through the collisional energy transfer, we can observe the satellite lines of $\Delta J'' \geq 40$, which may be depopulated by several times of collisions. More extensive studies including more accurate measurement of the lineshape are necessary in order to derive more information about the collisional process.

Acknowledgements

This work is supported by a Grant-in-Aid for Specially Promoted Research from the Ministry of Education, Science and Culture of Japan. S. K. thanks the Fellowship of the Japan Society for the Promotion of Science for Japanese Junior Scientists.

References

1. M. E. Kaminsky, R. T. Hawkins, F. V. Kowalski and A. L. Schawlow, Phys. Rev. Letters, *36*, 671, 1976.
2. R. Teets, R. Feinberg, T. W. Hänsch and A. L. Schawlow, Phys. Rev. Letters, *37*, 683, 1976.
3. N. W. Carlson, A. J. Taylor, K. M. Jones and A. L. Schawlow, Phys. Rev. Letters, *A24*, 822, 1981.
4. M. Raab, G. Höning, W. Demtröder and C. R. Vidal, J. Chem. Phys., *76*, 4370, 1982.
5. R. E. Teets, F. V. Kowalski, W. T. Hill, N. Carlson and T. W. Hänsch, Proceedings of the Society on Photo-optical Instruments and Engineering, San Diego, 1977, p. 88.
6. S. Kasahara, H. Ikoma and H. Katô, J. Chem. Phys., *100*, 63, 1994.
7. A. J. Ross, C. Effantin, J. d'Incan and R. F. Barrow, Mol. Physics, *56*, 903, 1985.
8. I. Kovács, Rotational Structure in the Spectra of Diatomic Molecules, Adam Hilger, London, 1969.
9. R. B. Kurzel, J. I. Steinfeld, D. A. Hatzenbuhler and G. L. Leroi, J. Chem. Phys., *55*, 4822, 1971.
10. Ch. Ottinger and D. Poppe, Chem. Phys. Letters, *8*, 513, 1971.
11. T. L. D. Collins, A. J. McCaffery, J. P. Richardson and M. J. Wynn, Phys. Rev. Letters, *70*, 3392, 1993.
12. H. Katô, S. R. Jeyes, A. J. McCaffery and M. D. Rowe, Chem. Phys. Letters, *39*, 573, 1976.
13. J. Derouard, H. Debontride, T. D. Nguyen and N. Sadeghi, J. Chem. Phys., *90*, 5936, 1989.